Science Press

Journal of Arid Land

2011, 3(3): 191–198

doi: 10.3724/SP.J.1227.2011.00191

jal.xjegi.com; www.chiansciencejournal.com

Magnetic property of loess strata recorded by Kansu profile in Tianshan Mountains

Jia JIA[1], XianBin LIU[1], DunSheng XIA[1,2*], HaiTao WEI[1], Bo WANG[1]

[1] Key Laboratory of West China's Environmental Systems (Ministry of Education), College of Earth Sciences and Environments , Lanzhou University, Lanzhou 730000, China;

[2] Key Laboratory of Desert and Desertification, Cold and Arid Regions Environmental and Engineering Research Institute, Chinese Academy of Sciences, Lanzhou 730000, China

Abstract: Kansu (KS) profile is located in the east of Yili basin, western Xinjiang, where typical loess sediments are distributed. The magnetic parameters (such as *IRM*, *SIRM SOFT*, and *M*) and grain size in the KS profile were analyzed in the study. The results showed that the magnetic property of KS loess is dominated by ferrimagnetic minerals, such as magnetite and maghemite. Antiferromagnetic and superparamagnetic minerals also exist in the profile, but had less impact on magnetic susceptibility. Compared with the typical loess sediments of the central Loess Plateau in China, the strata of Kansu profile contained more magnetic minerals and hard magnetic minerals. The analysis of grain size for magnetic minerals indicated that the properties of loess and paleosol were respectively dominated by PSD/MD and coarse SSD magnetite. The research found that the contents of magnetic minerals in loess and paleosol sequences in Kansu profile were similar, but the proportion of fine grained magnetite and soft magnetic minerals were varying, which implies a positive relationship between the value of magnetic susceptibility and intensity of pedogenesis.

Keywords: loess sediment; magnetic properties; pedogenesis; Kansu profile; Tianshan Mountains

In the Loess Plateau of China, loess/paleosol has been identified as an ideal carrier of paleoclimate signal (Heler and Liu, 1984; Kukla *et al*., 1988; Zhou *et al*., 1990; Liu *et al*., 1990, 1991; Maher and Thompson, 1991). Furthermore, the microscopy, geochemical and magnetic data from loessial soil layers across the Loess Plateau indicated the positive relationship between magnetic susceptibility and pedogenesis intensity (Heler and Liu, 1984; Kukla *et al*., 1988; Liu *et al*., 1990; Zhou *et al*., 1990; Maher and Thompson, 1991). Therefore, the magnetic susceptibility has been used as a valuable proxy of paleoclimate. However, the enhancement of susceptibility of the Chinese loess/paleosol sequences has been debated, and previously interpreted in terms of several mechanisms, e.g., depositional dilution of a constant flux of tropospheric ultrafine magnetic particles during glacial periods (Kukla *et al*., 1988), physical enrichment of magnetic minerals in paleosols due to decalcification and soil compaction (Heler and Liu, 1984), and pedogenic production of superparamagnetic particles (Liu *et al*., 1990; Zhou *et al*., 1990; Maher and Thompson, 1991; Meng *et al*., 1997). Furthermore, the mechanism that magnetic susceptibility is enhanced by the pedogenic formation of ultrafine, superparamagnetic and single domain grains of strongly magnetic iron oxide, magnetite in soil layers has been supported by more and more evidence (Heller and Evans, 1995; Liu *et al*., 2004; Deng *et al*., 2005).

The aeolian loess deposition is widely distributed in Northern Xinjiang where the magnetic properties have been investigated (Ye, 2001a, b; Shi *et al*., 2007). The different phenomenon had been discovered in Yili loess which showed negative relationship between χ_{lf} values and intensity of pedogenesis. It had given us much interest to do more detailed work to study the

Received 2011-03-15; accepted 2011-04-09

* Corresponding author: DunSheng XIA (E-mail: dsxia@lzu.edu.cn)

Yili loess. Yili basin is located in the west of Xinjiang, where the climate is dominant by the prevailing westerly atmospheric circulation and local wind regime. Pre- vious researches had indicated the differences of loess sediments between Yili area and Loess Plateau, and analyzed the mechanism of enhancement for magnetic susceptibility (Ye, 2001a, b). The viewpoint could explain the parallel variation between magnetic susceptibility and calcium carbonate concentration, however, the properties of magnetic minerals of loess deposition were not analyzed. The aim of the study is to investigate the relationship between magnetic properties and environment in the typical loess and paleosol sequences of Yili loess.

1 Study area

Loess deposition is usually distributed upon river terrace, while most of loessial soils were influenced by underground water in Tianshan Mountains. The typical loess in Tianshan Mountains was deposited in Kansu (KS) area which is locating in the upstream of the Gongnaisi River (Fig. 1) and is an ideal study area of magnetic implication. Furthermore, due to similar precipitation and temperature with the Loess Plateau, it is more significant to investigate the magnetic properties in this region. KS profile (43°31′N, 83°18′E) includes two segments which have been marked as KS1 and KS2.

The KS profile can be divided into seven soil layers which include two loess layers, three paleosol layers and one weak developed soil layer and one modern soil layer (Fig. 2). The modern soil layer is thin with discontinuity. By comparison within the profile, it can be concluded that upper loess layer was formed during the glacier period (corresponding Malan loess, marked by L_1), and the other layers were formed during the interglacial period (marked sequencely by S_1S_1, S_1L_1, S_1S_2, S_1L_2 and S_1S_3). L_1 loess layer is 3.74 m in thickness, with light yellow, uniform texture and loose structure. S_1S_1 layer is 1 m in thickness, with dark grey, uniform texture, compact structure and filled white mycelia. S_1L_1 is 1 m in thickness, with weak genesis, grey, uniform texture, compact structure, filled less white mycelia and some snail. S_1S_2 is 1 m in thickness in KS1 and 1.2 m in KS2, respectively, with dark grey, uniform texture, compact structure and filled white mycelia. S_1L_2 is 1.2 m, with light yellow, uniform texture, compact structure, filled less white mycelia and many snails. S_1S_3 is 1.42 m in thickness, with dark grey, uniform texture, compact structure, filled white mycelia.

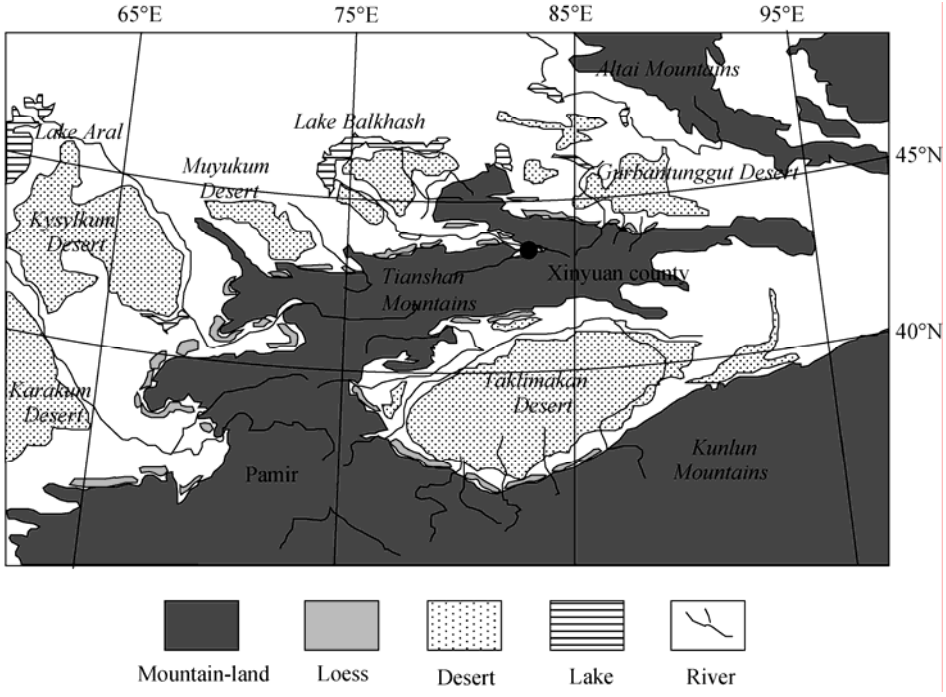

Fig. 1 The geographical location of the study area

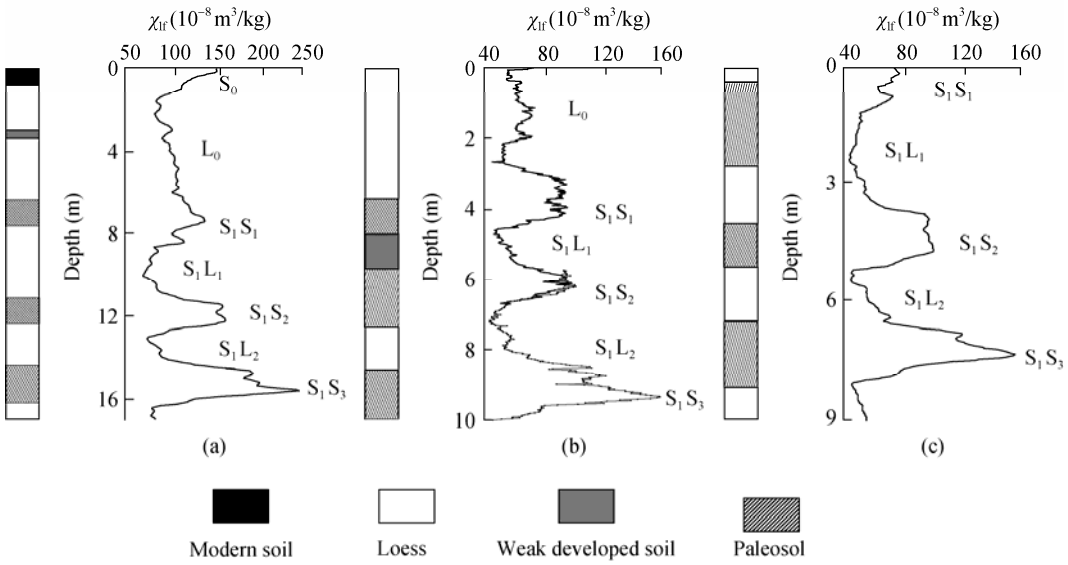

Fig. 2 Regional correlation of paleosol and loess sequences over Yili area. (a) and (c) are magnetic susceptibility curves (Ye *et al*., 2001a; Shi *et al*., 2007); (b) is magnetic susceptibility of KS profile.

2 Materials and methods

Total 561 samples were collected in KS profile at 2-cm interval. The samples are powder and not oriented. After air-drying in laboratory, 5.5-g powder for each sample was packed into plastic box for the following series of magnetic measurements: Low field (470 Hz) and high field (4,700 Hz) magnetic susceptibilities were measured by a Ms2 magnetometer (Bartington, England). Selected magnetic parameters are listed in Table 1. χ_{fd} and χ_{fd}% were calculated by the following equations: $\chi_{fd} = \chi_{lf} - \chi_{hf}$ and $\chi_{fd}\% = \chi_{fd}/\chi_{lf} \times 100\%$. *ARM* was measured by a DTECH AF demagnetizer with a peak AF field of 50 mT and DC bias field of 0.05 mT. In addition, χ_{ARM} was calculated. In this study, *IRM* acquired in the field of 1000 m (IRM 1000mT) was referred to as *SIRM*. *IRMs* and *SIRM* were imparted by an MMPM10 pulse magnetizer. All remanence measurements were made by a Minispin magnetometer. Stepwise backfield remagnetization of *SIRM* was carried out, and the result had been used to calculate *Hcr* by linear interpolation. After commonly experiments, we chose the representative samples to make further measurements: magnetic hysteresis loops (loops) and thermomagnetic curves (J-T curve) were determined using a variable field translation balance (VFTB) (Heating/cooling cycles which are measured from 25°C to 700°C in 110 mT magnetic field performed in air).

Table 1 Selected magnetic parameters

Abbr.	Parameters	Abbr.	Parameters
SP	Superparamagnetic particles	*IRM*	Isothermal remanent magnetization
SD	Single domain particles	*SIRM*	Saturation isothermal remanent magnetization
Coarse SSD	Coarse stable single domain particles	*Hcr*	Coercive force of remanence
PSD	Pesudo-single domain particles	*Hc*	Coercive force
MD	Multidomain particles	*M*	Saturation isothermal magnetization
χ_{lf}	Low-frequency magnetic susceptibility	M_{Max}	Max value of isothermal magnetization
χ_{fd}	Frequency-dependent magnetic susceptibility	M_0	Initial value of isothermal magnetization
$\chi_{fd\%}$	Percentage of frequency-dependent magnetic susceptibility	*Ms*	Saturation isothermal magnetization
χ_{ARM}	Anhysteretic susceptibility	*Mrs*	Saturation isothermal remanent magnetization
ARM	Anhysteretic remanent magnetization	*SOFT*	Isothermal remanent magnetization of soft magnetic particles

3 Results

3.1 Magnetic mineral

The loess samples (Fig. 3a) and paleosol (Fig. 3e) are all nearly saturated after magnetic field reached 300 mT, which indicates that the dominant component is ferrimagnetic mineral (Thompson and Oldfield, 1986). Furthermore, *IRM* curve enhancement of loess

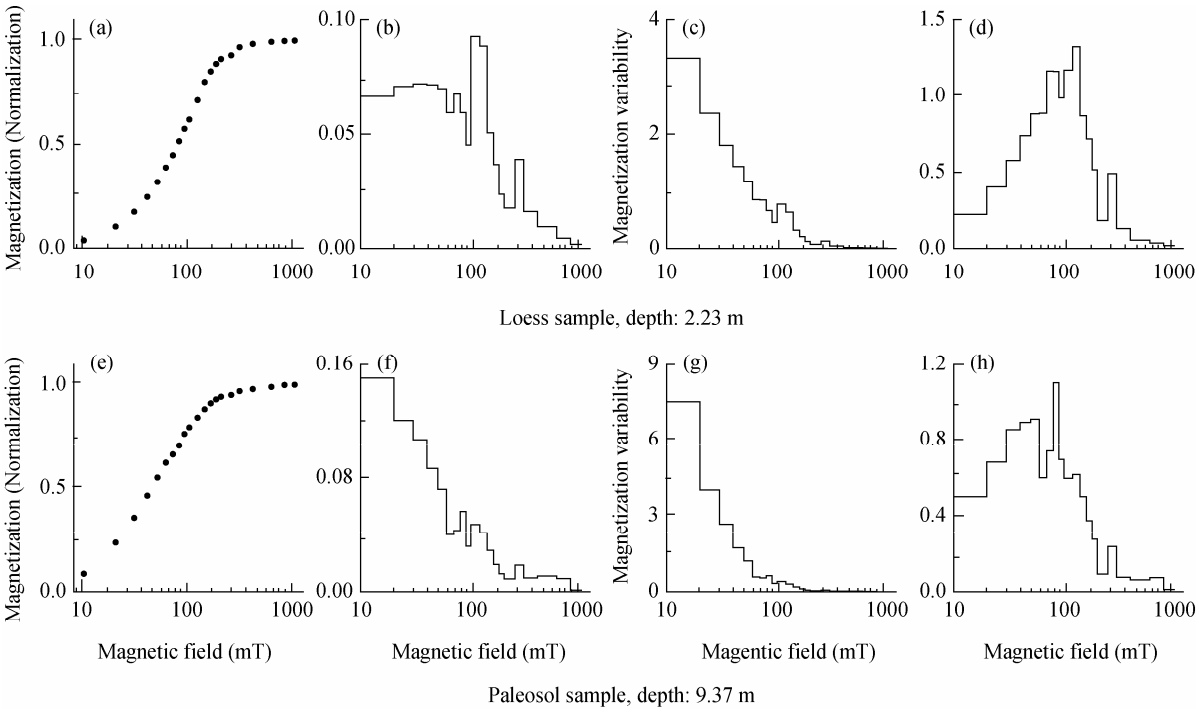

Fig. 3 The corrlation of *IRMs* curves between typical paleosol and loess of KS profile

(Fig. 3a) is more marked than that of paleosol (Fig. 3e). In addition, *IRM* of paleosol sample (Fig. 3f) enhances most obviously when the magnetic field is between 10 mT and 60 mT, which is lower than that of loess (Fig. 3b). All the samples show most obviously variability between 10 mT and 40 mT by magnetism curves, however, the value is larger in paleosol (Fig. 3g). By replacing normal magnetic field by logarithmic one, the peak of magnetic variation curves would be more wide, and then the peak of loess sample is more close to high magnetic field (Fig. 3h). These evidences indicate that paleosol contains more soft magnetic mineral particles.

Hysteresis properties of loess deposits can be used to indicate the magnetic phase of mineral (Thompson and Oldfield, 1986). As shown in Fig. 4, the magnetization of all samples increased sharply when the magnetic field was below 300 mT, and then the loops were nearly close at 300 mT in all cases, indicating a predominance of ferrimagnetic phase (Fig. 4), which supports the conclusion having been obtained from *IRM* curves (ferrimagnetism is the most important magnetic mineral in Yili area). From the contrasting values of *Ms*1 and *Ms*2, it can be observed that loess sample contains more paramagnetic mineral particles than paleosol.

High temperature magnetic properties are sensitive to mineralogical changes during thermal treatment, and such changes could provide credible information about magnetic mineral composition (Thompson and Oldfield, 1986; Deng *et al*., 2007; Liu *et al*., 2007a). The results show that magnetization of all samples is decreased quickly around 120°C which is the Curie point temperature of goethite (Fig. 5). The same phenomenon also occurred above 300–450°C, which is commonly in thermomagnetic curve of loess deposition and has been observed as the conversion of coarse-grained maghemite to hematite (Liu *et al*., 2007c, d). The heating lines of all samples show an obvious Curie point at 580°C, which suggests that magnetite dominates the high-temperature properties of these samples. The magnetization did not reach zero at 640°C in heating line, which is a signal of hematite. While, since hematite can be generated in heating process, it is hardly to judge whether it is a primary mineral.

As shown in Table 2, *Ms*, which is a parameter to measure the concentration of magnetic mineral is higher in Yili area than that in Xifeng (Thompson and Oldfield, 1986). Additional, the number of hard magnetic mineral, indicating by *Hc* and *Hcr*, is also higher in KS profile than that in Xifeng area (Zhu *et al*., 1994).

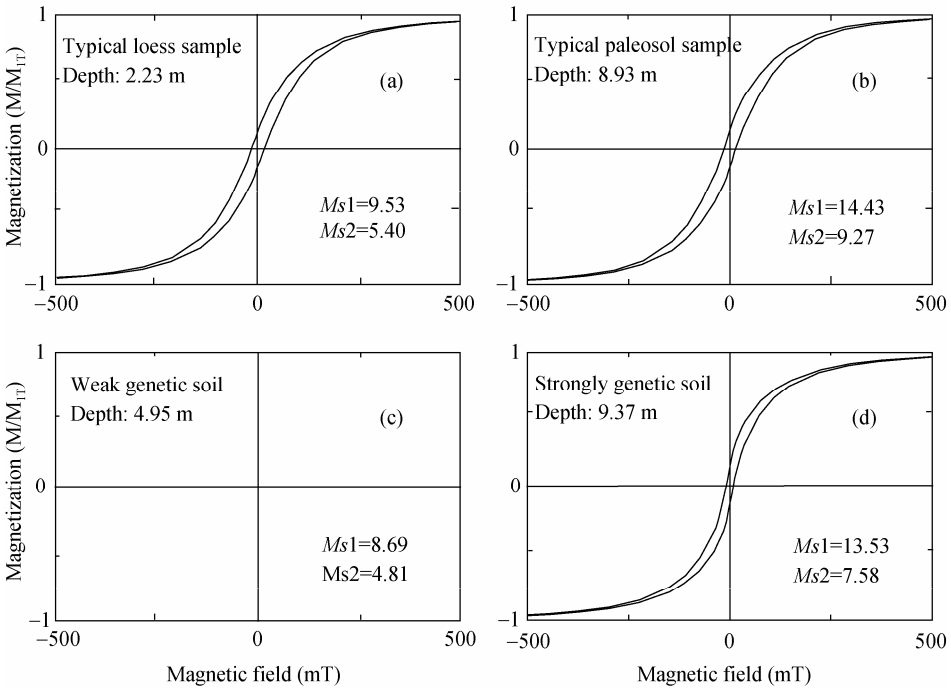

Fig. 4 Magnetic hysteresis loops of the typical samples in KS profile
(*Ms*1: the magnetization in 1T; *Ms*2: the magnetization of corrected for paramagnetism in 1T)

3.2 Grain size of magnetic mineral

Day-plot and Dearing-plot are two methods to analysis the grain size of magnetic mineral (Day *et al*., 1977; Dearing *et al.*, 1997; Dunlop, 2002). The results by Day-plot for the selected samples of KS profile indicate that MD/PSD grained magnetic mineral dominate the properties of loess deposition (Fig. 6). This conclusion is supported by Dearing-plot analysis which also indicates that most samples are MD/PSD grained magnetic minerals, and some of soil samples are Coarse SSD in KS profile.

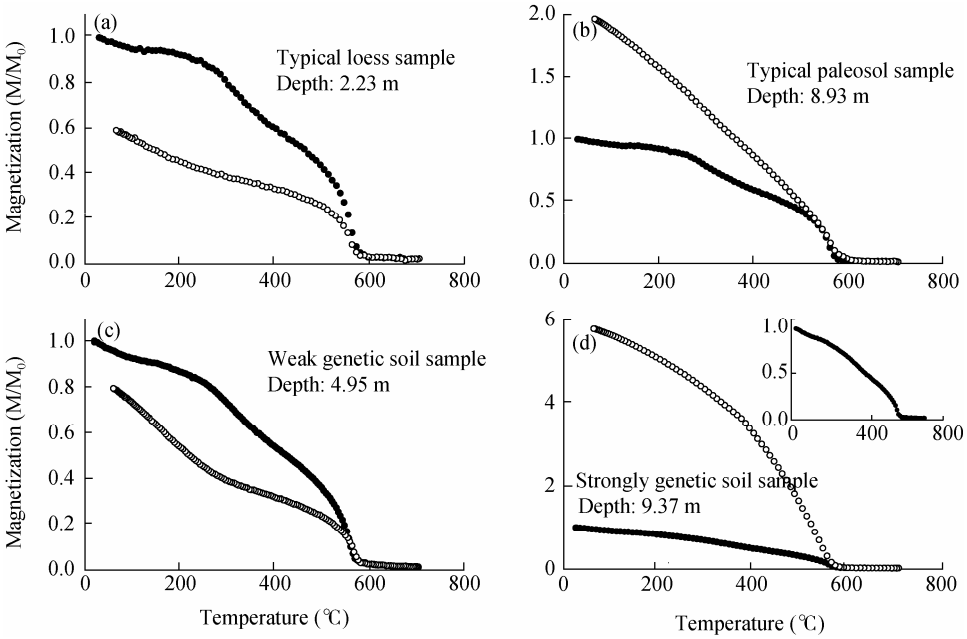

Fig. 5 M-T curves of the typical samples in KS profile (Filled circle: heating line, open circle: cooling line)

Table 2 Magnetic parameters comparison of typical loess and paleosols from Xifeng and Yili areas

Loess/paleosol	χ_{lf} (10^{-8} m^3/kg)	$\chi_{fd\%}$ (%)	χ_{ARM} (10^{-8} m^3/kg)	*Ms* (10^{-5}Am^2/kg)	*Mrs* (10^{-5}Am^2/kg)	*Hc* (mT)	*Hcr* (mT)
Xifeng loess	26.20	2.15		3,050.00	427.00	9.40	57.00
Xifeng weak pedogentic soil	58.50	5.43		5,510.00	771.40	7.70	35.00
Xifeng soil	134.90	9.66		9,940.00	1,590.40	5.60	30.00
Kansu typical loess	54.09	1.51	95.71	8,592.26	874.80	15.11	66.08
Kansu weak pedogentic soil	50.36	3.61	131.18	8,689.06	743.17	13.46	62.25
Kansu typical soil	107.58	2.82	240.00	13,006.53	1,632.02	13.74	61.80
Kansu strong pedogentic soil	159.15	8.14	651.13	12,193.99	1,362.42	8.81	42.75

Note: Xifeng data were form Liu *et al*. (2007c).

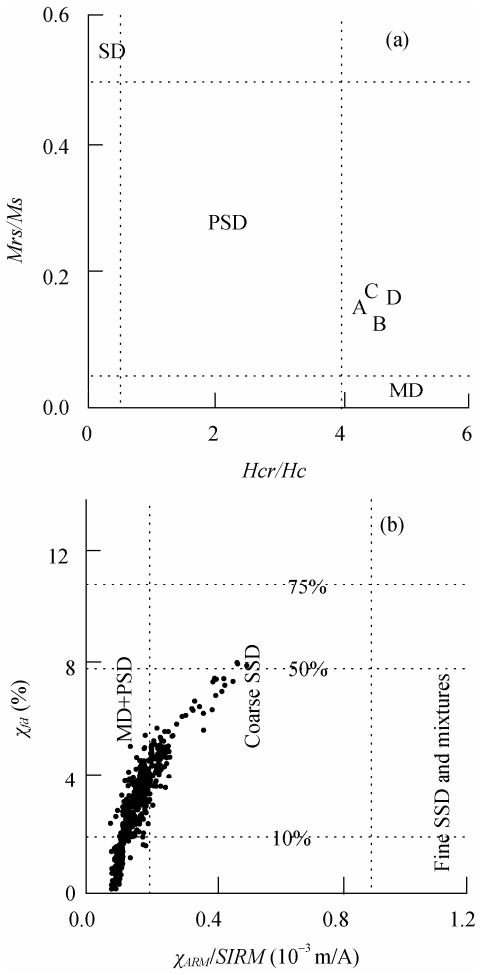

Fig. 6 Day-plot and Dearing-plot of typical loess and paleosol samples in KS profile, A: Typical loess; B: Great pedogenesis loess; C: Typical paleosol; D: Great pedogenesis paleosol.

The χ_{fd} value of S_1S_3 layer is obviously higher than that of other soil layers, however, their *SIRM* values are similar (Fig. 7), which indicates the similar concentration of magnetic minerals among the soil layers. On the other hand, the fine grained magnetic minerals in S_1S_3 are obviously increased. χ_{fd} is preferentially sensitive to a fairly narrow grain size range near the SP/SD (20–25 nm for magnetite) boundary (Liu *et al*., 2007a, b). Previous researches observed that the grain size distribution (GSD) of the SP+SD particles was fairly uniform, and appeared almost independent of the degree of pedogenesis (Liu *et al*., 2007b). Therefore, the concentration of SP and SD grained magnetic minerals is higher in S_1S_3 soil layers than that in other soil layers.

4 Discussion

Many hypotheses about magnetic susceptibility enhancement mechanism have been proposed to explain the variation of magnetic susceptibility in loess sediments, with high value in paleosol layers and low value in loess layers, such as physical enrichment of magnetic minerals in paleosol due to decalcification and soil compactness (Heler and Liu, 1984), depositional dilution of a constant flux of tropospheric ultrafine magnetic particles during glacier periods (Kukla *et al*., 1988), and pedogenic production of superparamagnetic particles (Liu *et al*., 1990; Zhou *et al*., 1990; Maher and Thompson, 1991). Although there were some debates, the pedogenic formation of ultrafine magnetic minerals can enhance the magnetic susceptibility of loess sediments which has been widely accepted.

However, Ye *et al*. (2001a, b) proposed that the magnetic susceptibility of pedogenic magnetic minerals is low because of the weak pedogenic soil layers in Yili area. By contrasting with $CaCO_3$ curve, Ye *et al*. (2001a, b) considered that variation of magnetic susceptibility was controlled by $CaCO_3$ concentration.

The negative correlation is displayed between magnetic susceptibility and $CaCO_3$ concentration, and the correlation coefficient is about –0.7392 (Fig. 8d), similar to Ye *et al*. (2001b), which supports that mag-

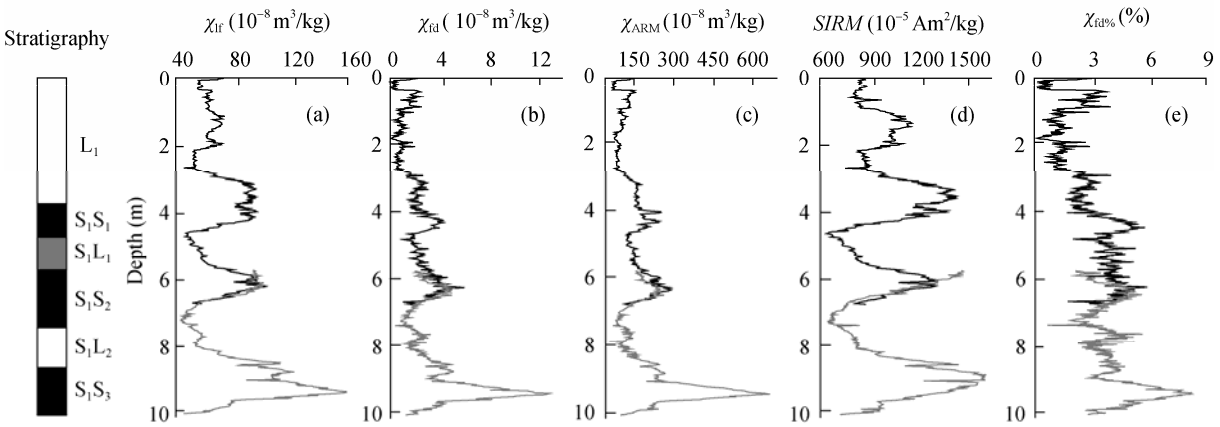

Fig. 7 The lithostratigraphy and common mineral magnetic parameters. (black line means KS1 section; grey line means KS2 section)

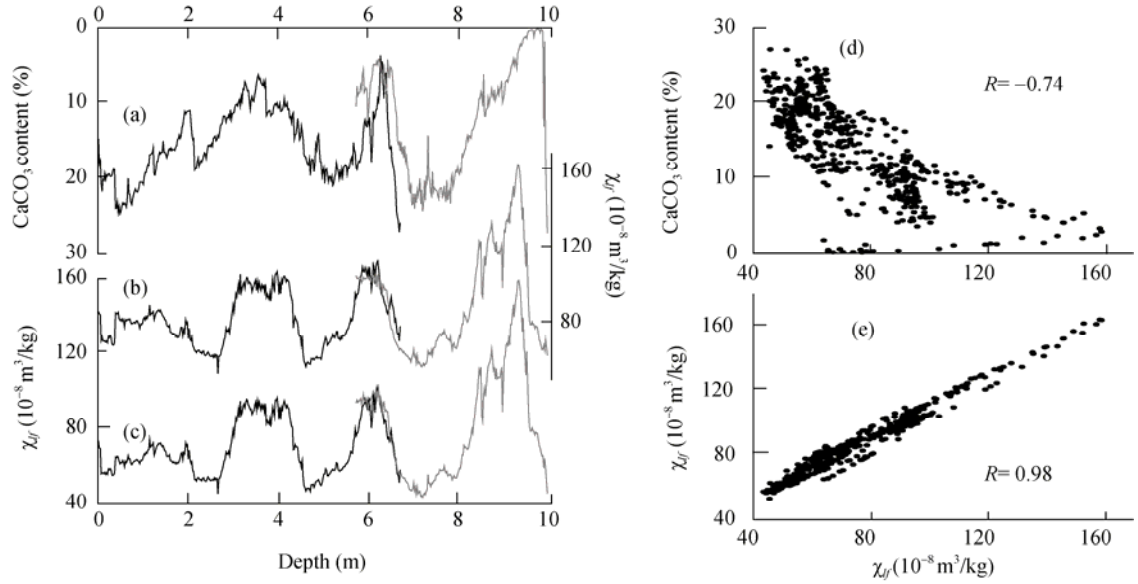

Fig. 8 The curves of χ_{lf}, χ_{lf} without $CaCO_3$ and with $CaCO_3$, and their correlation analyses

netic susceptibility is controlled by $CaCO_3$ concentration in Yili area. However, when $CaCO_3$ was removed, the magnetic susceptibility curve has no marked variation, and the correlation coefficient is 0.9838 (Fig. 8e), which means that $CaCO_3$ concentration is not the main controlling factor of magnetic susceptibility.

If the variation of magnetic susceptibility is controlled by $CaCO_3$ concentration, the difference of magnetic properties just occurs based on the density of magnetic minerals, not on magnetic properties of magnetic minerals. *SIRM* is a parameter to indicate the concentration of magnetic minerals. Although the range of χ_{lf} values is different among soil layers, the range of *SIRM* values is similar. This phenomenon is hardly explained by $CaCO_3$ decalcification. χ_{ARM} is a parameter indicating SD grained magnetic mineral (Thompson and Oldfield, 1986). Comparing χ_{ARM} with χ_{lf} curves, it is clear that the high fine grained magnetic minerals occur in soil layers. *Hcr* is a parameter to measure *SOFT* magnetic mineral concentration, which is a proxy of pedogenic intensity and is higher in paleosol layers than that in loess layers (Fig. 7). The results of *Hcr*, *SOFT* and χ_{lf} curves indicate that the content of pedogenic magnetic minerals is higher in soil layers than loess layers.

The investigation of magnetic properties for Xinjiang surface samples (Wei *et al*., 2009) showed that the average χ_{lf} value is 72.19×10^{-8} m^3/kg and $\chi_{fd\%}$ is

2.43%, which are obviously lower than that of loessic soil layers in Yili area. Therefore, the pedogenic magnetic minerals have higher magnetic susceptibility than the primary magnetic minerals. These are documented by the increase of χ_{fd}%, χ_{ARM}/χ and $\chi_{ARM}/SIRM$ values, which are the parameters of fine grained magnetic minerals.

5 Conclusion

The magnetic properties of loess sediments are similar between Yili area and Loess Plateau, which are all dominated by ferromagnetic minerals and less influenced by antiferromagnetic minerals. The magnetite and maghemite are two most important magnetic minerals in loess sediments of Yili area. However, it showed a higher concentration of ferrimagnetic mineral and hard mineral in Yili area than that in Loess Plateau loess. The result of grain size analysis showed that PSD/MD grained magnetic mineral was a dominating magnetic component of loess sediments in Yili area, while it was alternated by Coarse SSD grained magnetic mineral in some strongly pedogenic soil layers. The difference between loess and paleosoil layers showed more obvious in grain size than in concentration of magnetic minerals. Due to positive correlation between magnetic mineral grain size and pedogenic intensity, the parameters, such as $\chi_{fd\%}$, χ_{ARM}/χ and $\chi_{ARM}/SIRM$, are of great proxy to indicate the paleoenvironment and paleoclimate.

Acknowledgements

This study was funded by the National 973 Project (2009CB421308) and the Natural Science Foundation of China (40871080 and 90502008).

References

Day R, Fuller M, Schmidt V A. 1997. Hysteresis properties of titanomagnetites: grain-size and compositional dependence. Physics of the Earth and Planetary Interiors, 13(4): 260–267.

Dearing J A, Bird P M, Dann J L, *et al*. 1997. Secondary ferromagnetic minerals in Welsh soil: a comparison of mineral magnetic detection methods and implications for mineral formation. Geophysical Journal International, 130(3): 727–736.

Deng C L, Vidic N J, Verosub K L, *et al*. 2005. Mineral magnetic variation of the Jiaodao Chinese loess/paleosol sequence and its bearing on long-term climatic variability. Journal of Geophysical Research, 110: B03103, doi: 10.1029/2004JB003451.

Deng C L, Liu Q S, Pan Y X, *et al*. 2007. Environment magnetic of Chinese Loess. Quaternary Sciences, 27(2): 193–209.

Dunlop D J, Xu S, Heider F. 2004. Alternating field demagnetization, single-domain-like memory, and the Lowrie-Fuller test of multidomain magnetite grains (0.6–356 μm). Journal of Geophysical Research, 109: B07102, doi: 10.1029/2004JB003006.

Heller F, Liu T S. 1984. Magnetism of Chinese loess deposits. Geophysical Journal of Royal Astronomical Society, 77(1): 125–141.

Heller F, Evans M E. 1995. Loess magnetism. Reviews of Geoghysics, 33(2): 211–240.

Kukla G, Heller F, Liu X M, *et al*. 1988. Pleistocene climates in China dated by magnetic susceptibility. Geology, 16(9): 811–814.

Liu Q S, Jackson M J, Banerjee S K, *et al*. 2004. Mechanism of the magnetic susceptibility enhancements of the Chinese loess. Journal of Geophysical Research, 109, B12107, doi: 10.1029/2004JB003249.

Liu Q S, Deng C L, Pan Y X. 2007a. Temperature-dependency and frequency-dependency of magnetic susceptibility of magnetite and maghemite and their significance for environmental magnetism. Quaternary Sciences, 27(6): 955–962.

Liu Q S, Deng C L, Torrent J, *et al*. 2007b. Review of recent developments in mineral magnetism of the Chinese loess. Quaternary Science Reviews, 26(3–4): 368–385.

Liu X M, Liu T S, Heller F, *et al*. 1990. Frequency-dependent susceptibility of loess and Quaternary paleoclimate. Quaternary Sciences, 11(1): 42–50.

Liu X M, Liu T S, Heller F. 1991. The analysis of magnetic mineral's grain size in Chinese Loess and its paleoclimatic signification. Science in China: Series B, 21(6): 639–644.

Liu X M, Liu T S, Xia D S, *et al*. 2007c. The analysis of two different pedogenesis models in reductive and oxidative conditions record by Chinese and Siberia Loess. Science in China: Series D, 37(10): 1382–1391.

Liu X M, Xia D S, Liu T S, *et al*. 2007d. Discussion on two models of paleoclimatic records of magnetic susceptibility of Alaskan and Chinese loess. Quaternary Sciences, 27(2): 210–220.

Maher B A, Thompson R. 1991. Mineral magnetic record of the Chinese loess and palaeosols. Geology, 19(1): 3–6.

Meng X M, Derbyshire E, Kemp R A. 1997. Origin of the magnetic susceptibility signal in Chinese loess. Quaternary Science Reviews, 16(8): 833–839.

Shi Z T, Dong M, Fang X M. 2007. The characteristic of later Pleistocene loess-paleosol magnetic susceptibility in Yili Basin. Journal of Lanzhou University: Natural Sciences, 43(2): 7–10.

Thompson R, Oldfield F. 1986. Environmental Magnetism. London: Allen Unwin, 1–227.

Wei H T, Xia D S, Chen F H, *et al*. 2009. Magnetic characteristics of topsoil from Xinjiang, Northwestern China, and their implications. Frontiers of Earth Science in China, 3(3): 259–265.

Ye W. 2001a. Study on magnetic susceptibility of loess and palesol sequences in westerly region of Xinjiang. Journal of Desert Research, 21(4): 380–386.

Ye W. 2001b. The Loess Deposition Features and Paleoclimate in Westerly Region of Xinjiang. Beijing: Ocean Press, 108–124.

Zhou L P, Oldfield F, Wintle A G, *et al*. 1990. Partly pedogenic origin of magnetic variations in Chinese loess. Nature, 346: 737–739.

Zhu R X, Li C J, Wu H N, *et al*. 1994. Chinese loess property and its significance of paleoclimate. Science in China: Series B, 24(9): 992–997.